ChemComm

COMMUNICATION

View Article Online
View Journal | View Issue

Cite this: *Chem. Commun.*, 2025, **61**, 14641

Received 2nd May 2025,
Accepted 8th August 2025

DOI: 10.1039/d5cc02506k

rsc.li/chemcomm

Closed-loop recyclable cross-linked polymeric materials *via* dynamic transetherification

Pawan Kumar, †[a] Yashi Agarwal, †[a] Soumabrata Majumdar [b] and Ramkrishna Sarkar ‡*[a]

This work communicates the closed-loop recyclability and dynamic property tunability in benzylic ether-based cross-linked polymers. Remarkably, the polymers were fully degradable *via* transetherification, and the monomers were recovered in high yields. The recovered monomers were used to re-synthesize the polymers with pristine-like material properties. Further on, the tunability of dynamic properties was investigated by a systematic increase in the inter-crosslink distance by four methylene groups, which showed strong effects on the stress relaxation property.

Covalent adaptable networks (CANs), a class of dynamically cross-linked polymers, have emerged as a promising alternative to traditional thermoset polymers.[1,2] Owing to the presence of dynamic covalent bonds that undergo exchange upon activation by an external stimulus, CANs are reprocessable like thermoplastics while maintaining thermoset-like properties in the target application conditions. A variety of dynamic bonds have been introduced to tailor the polymers with specific and desired characteristics.[3–13] Designing chemistries that impart both robustness and dynamicity to polymer networks is a key challenge. There have been a few literature reports focused on designing robust CANs based on chemistries such as siloxane exchange, thiol–yne, dynamic enamine-urea linkage, and reversible alkoxyamine.[14–17] Expanding the scope further, we have recently introduced transetherification on benzylic ethers to this list of thermally robust dynamic chemistries.[18]

Besides providing malleability upon activation, dynamic linkages in a cross-linked polymer can also enable its chemical recycling in a closed-loop fashion, offering a solution to the challenges associated with the end-of-life management of these materials.[19–23] The recovered monomers upon chemical recycling can be used to regenerate the original polymers, retaining their original quality and properties, or can be used to produce value-added monomers and materials, offering a scope for upcycling.[24–26] Recent efforts in closed-loop recyclability have focused on dynamic linkages such as diketoenamine exchange, imine, transesterification, transimination, and reversible amidation.[27–29] Despite these advancements, the range of dynamic covalent motifs employed thus far remains limited compared to the extensive library of dynamic chemical reactions available. Moreover, designing dynamic bonds that enable effective bonding, robustness, and reversible cleavage for monomer generation remains a significant challenge in developing closed-loop recyclable cross-linked polymers.

Here, we demonstrate the closed-loop recyclability of the CANs using our recently developed trans-ether exchange as a robust chemistry, a dynamic covalent chemistry.[18] The networks were degraded chemically, and monomers were recovered with high yields. The recovered monomers were utilized to prepare a fresh polymer with near retention of its properties, thus enabling closed-loop recyclability. Additionally, we re-establish our previous claim of dissociative bond exchange in benzylic ethers with more rigorous model compound studies. Furthermore, the effect of crosslink density on the dynamic property of these networks has also been explored. Compared to CANs showing associative bond exchange, the effect of network structure on the dynamic properties has much less been studied for dissociative CANs, especially the ones that require an external catalyst for bond exchange, like the benzylic ethers.[30–32] Here we have prepared networks by systematically varying the inter-crosslink distance by four methylene units and studied the effect of crosslink density on the thermo-mechanical and dynamic properties of the networks.

A tri-benzyl ether containing molecule 1,3,5-tris(methoxymethyl)-2,4,6-trimethylbenzene (**TMM-TMB**), to be used as the crosslinker in the network, was synthesized from mesitylene in two steps (Scheme 1a). In brief, first, the chloromethylation of mesitylene was carried out to obtain 1,3,5-tris(chloromethyl)-2,4,6-trimethylbenzene (**TCM-TMB**). **TCM-TMB** was subsequently

[a] *Department of Chemistry, Indian Institute of Technology Kanpur, Kanpur, Uttar Pradesh, 208016, India. E-mail: ramkrishna@iitk.ac.in*
[b] *Physical Chemistry and Soft Matter, Wageningen University and Research, Wageningen, 6700 HB, The Netherlands*
† Authors contributed equally.
‡ This work is dedicated to Prof. S. Ramakrishnan, IISc Bangalore, on the occasion of his 65th birthday.

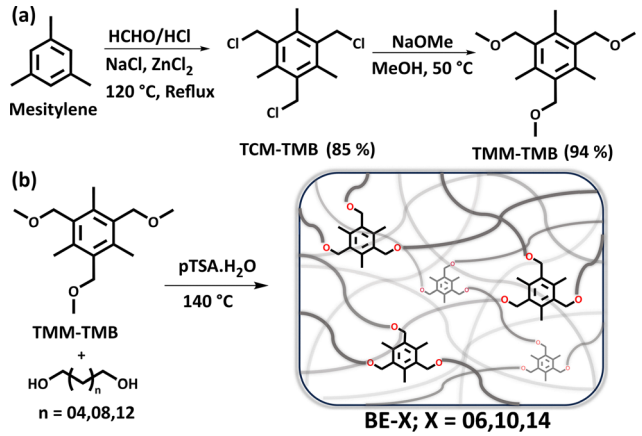

Scheme 1 (a) Synthesis scheme of tri-benzyl ether bearing monomer, **TMM-TMB**, starting from mesitylene. (b) Scheme showing the synthesis of the dynamic benzyl ether-based networks.

reacted with sodium methoxide to obtain **TMM-TMB** bearing the benzyl ether linkages. All the molecules were structurally characterized using ^{1}H and ^{13}C **NMR**, and **HR-MS** (Fig. S1–S6). Before network synthesis, model exchange studies were conducted to explore the mechanism and versatility of transetherification on benzylic ether. Exchange reactions were performed on **THM-TMB** with 2-(2-methoxyethoxy)ethanol (**MEE**) (Scheme S2 and Fig. S17, S18) at different temperatures, revealing an activation energy for the reaction of 165.96 kJ mol^{-1} (Fig. S19). The exchange was faster for primary alcohols than secondary alcohols, whereas the tertiary alcohols showed no significant exchange (Scheme S1 and Fig. S7–S16). Moreover, the exchange reaction was found to proceed with anhydrous pTSA also (Scheme S5 and Fig. S62, S63). Besides, the transetherification rates were independent of the alcohol concentration (Fig. S20–S22). This, along with other model studies, re-establishes the previously reported claim of dissociative exchange mechanism *via* benzylic carbocation intermediate (Schemes S3, S4 and Fig. S23–S26).

Upon successful affirmation of benzyl ether's exchangeability, the ether-based polymer networks were prepared by melt-transetherification using the trifunctional **TMM-TMB** and aliphatic diol (Scheme 1b). To regulate the properties of the polymers, a series of linear aliphatic diols with varying carbon segment lengths was utilized, namely 1,6-hexanediol, 1,10-decanediol, and 1,14-tetradecanediol. Thus, in each diol monomer, the methylene segment length was varied by 4 units. The corresponding benzyl ether (**BE**) bearing polymers were named **BE-06**, **BE-10**, and **BE-14**, respectively. Further molecular characterization of polymer networks was performed.[33,34] FT-IR studies suggested the formation of the polymers (Fig. S27–S29). All the networks showed high gel content (>90%) in DCM and THF (Table S1 and Fig. S30). Besides, the % weight swelling in both solvents was higher for the networks with higher diol spacer length because of reduced crosslink density (Table 1 and Fig. S31), which is in agreement with the crosslink density estimated using **DMTA** studies (Fig. S48).

The thermal stability of the networks was probed using thermogravimetric analysis (**TGA**). The temperature for 5% weight loss ($T_{d,5\%}$) was 294 °C, 300 °C, and 326 °C for **BE-06**, **BE-10**, and **BE-14** respectively (Table 1, Fig. 1a). The high $T_{d,5\%}$ values are in support of the claim of benzylic ethers being a robust dynamic moiety. The slight increase in thermal stability with increasing diol length can be attributed to the higher boiling points of the longer diols. Isothermal **TGA** at 200 °C for 3 hours showed a minimal weight loss (<3%) (Fig. S32), indicating excellent thermal stability and broader processing potential. Besides, the polymers were found to be stable in various chemicals as probed by gravimetry and **FT-IR** analysis (Tables S2, S3 and Fig. S33–S38). The glass transition temperature (T_g) of the networks was determined to be 53.50 °C, 12.78 °C, and −2.60 °C using differential scanning calorimetry (**DSC**) for **BE-06**, **BE-10**, and **BE-14**, respectively (Fig. 1c). The observed lowering of T_g with the increase in diol chain length could be attributed to the increased chain mobility in networks with lower crosslink density,[35] which is also supported by the decrease in rubbery plateau modulus in the temperature sweep profiles (Fig. 1b). Till temperatures below 200 °C, the benzylic ether-based networks did not show a drop in the storage modulus because of equilibrium shifting to the dissociated state, as is common for most other dissociative CANs. Furthermore, similar to the temperature sweep, the frequency sweep experiments also did not show any drop in modulus with increasing temperature (Fig. S45–S47). This could be due to the highly active dissociated state with a very low lifetime,

Table 1 The properties of networks

	Q_w (%) (DCM)	$T_{d,5\%}$ (°C) (TGA)	T_g (°C) (DSC)	E (MPa)	E_b (mm)	UTS (MPa)	E_a (kJ mol^{-1})
BE-06	70.6	294	53.50	86.83	7.60	10.94	119.8
BE-10	122.2	300	12.78	35.52	5.84	2.16	130.7
BE-14	134.8	326	−2.60	16.76	7.12	1.22	150.5

E: Young's modulus; E_b: elongation at break; UTS: ultimate tensile strength. E, E_b, and UTS were estimated using tensile test; Q_w: weight swelling; E_a: activation energy.

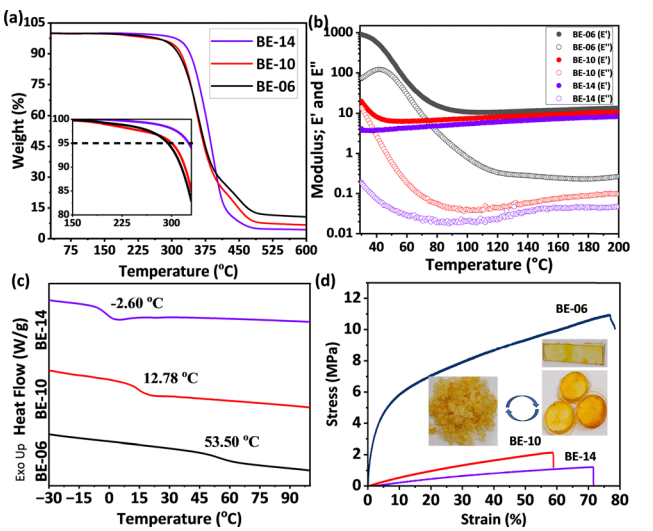

Fig. 1 (a) The **TGA** profiles of the networks. The inset shows zoomed TGA profiles. (b) DMTA, (c) DSC profile, and (d) tensile plots for networks. The inset shows the reprocessing of the **BE-14**.

similar to that previously reported by Du Prez and coworkers for internally catalyzed transesterification based dissociative CANs.[36]

The grounded polymer samples were successfully reprocessed into rectangular bars and disk-shaped specimens using compression molding at 170 °C under 10-ton pressure, owing to the active transetherification under these conditions (Fig. 1d inset). FT-IR analysis indicated that the polymer structure remained largely unchanged during reprocessing (Fig. S39–S41). The mechanical properties of the reprocessed polymer samples showed that both Young's modulus and ultimate tensile strength decreased with increasing diol chain length. Specifically, Young's modulus values for **BE-06**, **BE-10**, and **BE-14** were 86.83, 35.52, and 16.76 MPa, respectively (Fig. 1d and Table 1). Furthermore, tensile testing of the 2nd reprocessed samples (reprocessing of the first reprocessed sample) revealed mechanical properties, specifically Young's modulus and ultimate tensile strength, comparable to those of the first reprocessed samples (Fig. S50). A slight reduction in elongation at break was noted, which may be attributed to increased microstructural defects.[36]

As the polymers are composed of dynamic ether linkages, they showed relaxation of imposed stresses at elevated temperatures, as can be seen in Fig. 2a, Fig. S51, S52, and Table S4. The relaxation was faster at higher temperatures for a particular polymer due to the faster bond exchanges. At a fixed temperature, the relaxation was fastest in **BE-06** and slowest in **BE-14** (Fig. S53–S56). Further, the activation energies (E_a) of **BE-06**, **BE-10**, and **BE-14** were estimated to be 119.8, 130.7, and 150.5 kJ mol^{-1}, respectively (Fig. 2b). The benzylic ether dissociation in the network involves an external catalyst. The increase in spacer length from **BE-06** to **BE-14** leads to a reduced effective catalyst concentration in the matrix, potentially causing the observed slower relaxation and higher activation energy, consistent with previously reported studies.[37–39] The networks' lower activation energy compared to the small-molecule model may result from activated transetherification. All rheological studies were conducted within the linear viscoelastic regime (LVR), estimated from strain sweep experiments (Fig. S42–S44).

After demonstrating the robustness and dynamic behavior of the polymers, with the aim of regenerating the monomer, the degradation was carried out using methanol (Fig. 3a). All the networks were shown to degrade completely and form a

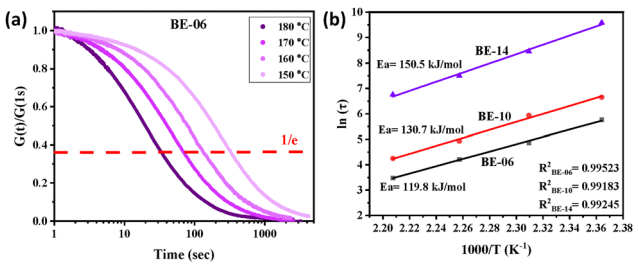

Fig. 2 (a) The normalized (at t = 1 s) stress relaxation profile of **BE-06**, ranging from 150 °C to 180 °C. (b) Activation energy plot.

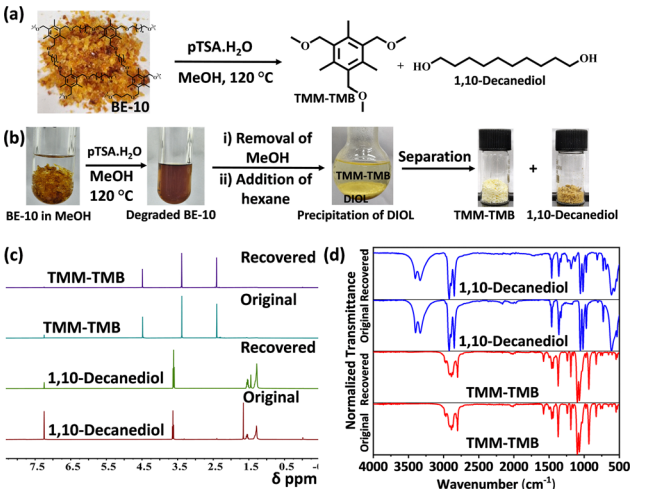

Fig. 3 (a) Scheme of **BE-10** degradation using methanol. (b) Pictorial representation of the degradation of **BE-10** and the recovery of the monomers, (c) ^{1}H **NMR** and (d) **FT-IR** comparison of the original and recovered monomers.

homogeneous solution when heated in excess methanol in the presence of pTSA·H_2O for 12–16 hours at 120 °C (Fig. 3b). The monomer mixtures were obtained after the removal of methanol. The addition of the hexane to this mixture resulted in the selective precipitation of the diol and solubilization of the triether monomer, **TMM-TMB**. Thus, employing the polarity difference, the monomers could easily be separated. Both monomers were recovered with high yield. For instance, **TMM-TMB** and 1,10 decanediol were recovered with >96% and >93% yield, respectively, from **BE-10**. The monomers were recovered with good yield for the other two networks, **BE-06** and **BE-14**, as well. Degradation was performed three times for all networks, and the average monomer recovery was estimated (Table S5). The degradation *via* depolymerization was feasible due to the presence of dynamic ether linkages, where the participation of the excess methanol in the transetherification resulted in the disintegration of the polymer network. The comparison of the ^{1}H NMR and FT-IR spectra of the pristine and recovered monomers showed that the monomers were recovered in good purity (Fig. 3c, d and Fig. S57, S58). The recovered monomers were repolymerized to prepare a fresh network **BE-10R**. **BE-10**, being in the middle of the series, was selected for this study. A comparison of the properties of the recycled network, **BE-10R**, with the pristine network, **BE-10**, revealed that their material properties were comparable (Fig. S59 and S61). This demonstrates the retention of material characteristics upon recycling.

In summary, the dynamic properties of the CANs were regulated systematically by varying the inter-crosslink distance. The network with lower crosslink density showed slower stress relaxation and higher activation energy, likely due to catalyst dilution in the matrix. Interestingly, the relaxation rate dependence on crosslink density for the reported networks and also the temperature sweep profiles are more aligned with properties of vitrimers, associative CANs.[31,40] However, the model

studies clearly show a dissociative bond exchange mechanism, making this a system intermediate to classical associative and dissociative CANs from a macroscopic response point of view. Further on, the closed-loop recyclability of networks was demonstrated. Complete methanolysis of the networks regenerated the monomers, which were recovered with high yields. The networks synthesized from the recovered monomers showed similar properties to those of the pristine ones. To the best of our knowledge, this is the first study wherein transetherification chemistry has been employed to design closed-loop recyclable cross-linked polymers. By incorporating closed-loop recyclability into the cross-linked polyether materials, we anticipate unlocking new avenues for the design of sustainable materials.

The manuscript was written with contributions from all authors. All authors have approved the final version of the manuscript. Dr Kumar thanks IIT Kanpur for the postdoctoral fellowship. Ms YA thanks IIT Kanpur for the fellowship. Dr Sarkar thanks Science and Engineering Research Board (SERB), Department of Science and Technology, Government of India (Grant number: EEQ/2022/000078) for funding. The authors thank IIT Kanpur for the infrastructure.

Data availability

Data supporting this article have been included in the SI. Supplementary information: experimental section, characterization, kinetic study, stability study, rheological study, and polymer degradation. See DOI: **https://doi.org/10.1039/d5cc02506k**

Conflicts of interest

The authors declare no conflicts of interest.

Notes and references

1 S. Samanta, S. Kim, T. Saito and A. P. Sokolov, *J. Phys. Chem. B*, 2021, **125**, 9389–9401.
2 N. De Alwis Watuthanthrige, P. Chakma and D. Konkolewicz, *Trends Chem.*, 2021, **3**(3), 231.
3 D. Montarnal, M. Capelot, F. Tournilhac and L. Leibler, *Science*, 2011, **334**, 965–968.
4 P. Taynton, K. Yu, R. K. Shoemaker, Y. Jin, H. J. Qi and W. Zhang, *Adv. Mater.*, 2014, **26**, 3938–3942.
5 J. J. Cash, T. Kubo, A. P. Bapat and B. S. Sumerlin, *Macromolecules*, 2015, **48**, 2098–2106.
6 D. J. Fortman, R. L. Snyder, D. T. Sheppard and W. R. Dichtel, *ACS Macro Lett.*, 2018, **7**, 1226–1231.
7 W. Denissen, M. Droesbeke, R. Nicola, L. Leibler, J. M. Winne and F. E. Du Prez, *Nat. Commun.*, 2017, **8**, 14857.
8 P. Chakma and D. Konkolewicz, *Angew. Chem., Int. Ed.*, 2019, **58**, 9682–9695.
9 N. Zheng, Y. Xu, Q. Zhao and T. Xie, *Chem. Rev.*, 2021, **121**, 1716–1745.
10 S. K. Schoustra, T. Groeneveld and M. M. J. Smulders, *Polym. Chem.*, 2021, **12**, 1635–1642.
11 S. Chen, V. Scholiers, M. Zhang, J. Zhang, J. Zhu, F. E. D. Prez and X. Pan, *Angew. Chem., Int. Ed.*, 2023, **62**, e202309652.
12 R. Wink, S. Majumdar, R. A. T. M. van Benthem, J. P. A. Heuts and R. P. Sijbesma, *Polym. Chem.*, 2023, **14**, 4294.
13 L. T. Nguyen, F. Portone and F. E. Du Prez, *Polym. Chem.*, 2023, **15**, 11–16.
14 K. Jin, L. Li and J. M. Torkelson, *Adv. Mater.*, 2016, **28** 6746–6750.
15 Y. Nishimura, J. Chung, H. Muradyan and Z. Guan, *J. Am. Chem. Soc.*, 2017, **139**, 14881–14884.
16 N. Van Herck, D. Maes, K. Unal, M. Guerre, J. M. Winne and F. E. Du Prez, *Angew. Chem.*, 2020, **132**, 3637–3646.
17 S. Chen, J. Ding, Y. Zhao, A. Yuan, Y. Liao, X. Chen, Y. Lei, L. Jiang, J. Lei and X. Fu, *Macromolecules*, 2019, **52**, 1257–1265.
18 P. Kumar, V. Gupta, S. Majumdar, R. Patwal, D. Das, P. K. Ashish and R. Sarkar, *Chem. Commun.*, 2025, **61**, 5621.
19 P. R. Christensen, A. M. Scheuermann, K. E. Loeffler and B. A. Helms, *Nat. Chem.*, 2019, **11**, 442–448.
20 G. W. Coates and Y. D. Y. L. Getzler, *Nat. Rev. Mater.*, 2020, **5**, 501–516.
21 M. Häußler, M. Eck, D. Rothauer and S. Mecking, *Nature*, 2021, **590**, 423–427.
22 P. R. Maity, C. Upadhyay, A. S. K. Sinha and U. Ojha, *Chem. Commun.*, 2023, **59**, 4225.
23 V. Gupta and R. Sarkar, *J. Polym. Sci.*, 2025, **63**(10), 2237–2247.
24 C. Jehanno, J. W. Alty, M. Roosen, S. De Meester, A. P. Dove, E. Y. X. Chen, F. A. Leibfarth and H. Sardon, *Nature*, 2022, **603**, 803–814.
25 S. S. Rege, I. Dey, S. Vimal Kumar, N. Singh, A. Misra, K. Samanta and S. Bose, *ACS Appl. Polym. Mater.*, 2025, **7**(8), 4908–4917.
26 V. Gupta, S. Majumdar, D. Das, P. K. Ashish and R. Sarkar, *Polymer*, 2025, **328**, 128438.
27 K. Saito, F. Eisenreich, T. Türel and Ž. Tomović, *Angew. Chem., Int. Ed.*, 2022, **61**, e202211806.
28 B. Qin, S. Liu, Z. Huang, L. Zeng, J. F. Xu and X. Zhang, *Nat. Commun.*, 2022, **13**, 7595.
29 L. Sougrati, A. Duval and L. Avérous, *Chem. Eng. J.*, 2025, **511**, 162201–162215.
30 Y. Liu, Z. Tang, J. Chen, J. Xiong, D. Wang, S. Wang, S. Wu and B. Guo, *Polym. Chem.*, 2020, **11**, 1348–1355.
31 L. Koenig, K. M. Allis, J. S. Lehr and M. B. Larsen, *Polym. Chem.*, 2024, **16**, 52–61.
32 D. J. Fortman, J. P. Brutman, M. A. Hillmyer and W. R. Dichtel, *J. Appl. Polym. Sci.*, 2017, **134**, 44984–44993.
33 S. P. O. Danielsen, H. K. Beech, S. Wang, B. M. El-Zaatari, X. Wang, L. Sapir, T. Ouchi, Z. Wang, P. N. Johnson, Y. Hu, D. J. Lundberg, G. Stoychev, S. L. Craig, J. A. Johnson, J. A. Kalow, B. D. Olsen and M. Rubinstein, *Chem. Rev.*, 2021, **121**, 5042–5092.
34 C. W. H. Rajawasam, O. J. Dodo, M. A. S. N. Weerasinghe, I. O. Raji, S. V. Wanasinghe, D. Konkolewicz and N. De Alwis Watuthanthrige, *Polym. Chem.*, 2024, **15**, 219–247.
35 S. C. Lee and B. G. Min, *Polymer*, 1999, **40**, 5445–5448.
36 M. Delahaye, J. M. Winne and F. E. Du Prez, *J. Am. Chem. Soc.*, 2019, **141**, 15277–15287.
37 M. Capelot, M. M. Unterlass, F. Tournilhac and L. Leibler, *ACS Macro Lett.*, 2012, **1**, 789–792.
38 M. Hubbard, Y. Ren, D. Konkolewicz, A. Sarvestani, C. R. Picu, G. S. Kedziora, A. Roy, V. Varshney and D. Nepal, *ACS Appl. Polym. Mater.*, 2021, **3**, 1756–1766.
39 J. G. P. Rodrigues, S. Arias, J. G. A. Pacheco and M. L. Dias, *RSC Adv.*, 2023, **13**, 33613–33624.
40 M. Hayashi and R. Yano, *Macromolecules*, 2020, **53**, 182–189.

